Proceedings of
10th European Conference on Turbomachinery Fluid dynamics & Thermodynamics
ETC10, April 15-19, 2013, Lappeenranta, Finland

MODELLING UNSTEADINESSES AND POLYDISPERSION IN WET STEAM FLOWS USING THE QUADRATURE METHOD OF MOMENTS AND A TWO-EQUATION MODEL

F. Blondel - M. Stanciu

EDF R&D - Electricite de France, Chatou, France, frederic-f.blondel@edf.fr, mugurel.stanciu@edf.fr

F. Leboeuf - M. Lance

ECL - Ecole Centrale de Lyon - Ecully, France, francis.leboeuf@ec-lyon.fr, michel.lance@ec-lyon.fr

ABSTRACT

The efficient prediction of wetness and droplet size in steam turbine flows is still a challenge in Computational Fluid Dynamics nowadays. Most of the time, polydispersed models (i.e. numerous radii are considered) such as the sectional method, involve a large number of transport equations, and can be computationally unstable. In this paper, the polydispersed Quadrature Method of Moments (QMOM) is tested and compared with a classical, monodispersed (i.e. only one representative radius is considered) two-equation model. The use of the QMOM method is a step toward the description of the Particle Size Distribution in a context of large industrial CFD calculations: only a few equations are transported and a coarse distribution is computed. Academic test cases dealing with unsteadiness and shock wave instabilities in nozzles highlight the ability of the QMOM method to handle polydispersion and unsteadiness in flow fields similar to those encountered in steam turbines. The QMOM method has shown a very stable behaviour and proved to be a very good tool for condensation prediction in industrial applications.

NOMENCLATURE

A	nozzle cross-section	q_c	correction factor
c	sound speed	r	droplet radius (or abscissas)
c_p	specific heat at constant pressure	R_{H_2O}	water constant
e, E	static, total internal energy	s	entropy
f	particle size distribution function	t	time
F	fluxes	u	velocity
g	growth law	W	conservative variables
h, H	static, total enthalpy	w	weight
J	nucleation rate	x	position
L_h	latent heat	y	liquid mass fraction
m	mass of a droplet	Y	primitive variables
N	droplet number per unit mass of mixture	Kn	Knudsen number
p	pressure	Pr	Prandtl number

Sup- and Subscripts		Greek letters	
32, 2_{eq}	Sauter and average radius	β	correction factor
$\dot{}$	time derivative	δ	Dirac operator
*	single vapor molecule	γ	ratio of specific heats
c	critical size	Λ	thermal conductivity
int	intermediate state	λ	eigenvalue
m, g, l	mixture, gas, or liquid phase	μ	moment of a distribution
num	numerical	ν	specific volume
R, L	right, left	ψ	passive scalar
sat	saturation condition	ρ	mass density
$\tilde{},^{-}$	Roe average	σ	surface tension

INTRODUCTION

Steam condensation in power plants turbines is an important issue as it induces critical losses of efficiency and damages the turbine blades by erosion. This phenomenon is complex and depends on many parameters, such as non-equilibrium real gas effects, turbulence and flow unsteadiness. Therefore, realistic CFD simulations of condensing flows require many efforts. The use of efficient and advanced CFD models is of major concern, as it leads to a better understanding of the flow field in turbines. Currently, monodispersion of the droplet sizes is mainly considered. This hypothesis is strong, since it has been experimentally observed that the droplet size distribution is broad in steam turbines. But, taking polydisperson into account in an Eulerian frame of reference is often tricky, time consuming, unstable (White, 2003), and thus not yet feasible for large industrial calculations. In an industrial framework, the QMOM method looks like a good compromise between the full resolution of the particle size distribution and monodispersed models. The method is efficient, the number of transport equations is relatively low, and a coarse droplet spectrum is computed. QMOM was introduced by McGraw (1997), and applied to nucleating wet steam flows by Gerber and Mousavi (2007). But there are still some uncertainties on the ability of the QMOM method to handle unsteadiness and strong discontinuities. These issues are treated through academic validation cases in this paper, and compared with a less advanced, monodispersed two-equation model.

GOVERNING EQUATIONS

A one-dimensional code has been developed to solve unsteady, compressible, non-viscous flows of wet steam in nozzles. Single-fluid, mono-pressure models are considered here: the static pressure is the same for the gaseous phase and for the liquid phase. The velocity slip between phases is neglected, because droplets created during the nucleation process are tiny, less than 0.2 μm in radius, and are supposed to travel at the gaseous phase velocity. Viscous effects and heterogeneous condensation (condensation around existing nuclei) are also not taken into account for the moment.

Mixture model

Under the considerations exposed above, the governing equations for the mixture are written, in quasi-1D form (Anderson, 1995):

$$
\begin{aligned}
A\frac{\partial(\rho_m)}{\partial t} + \frac{\partial(\rho_m u_m A)}{\partial x} &= 0 \\
A\frac{\partial(\rho_m u_m)}{\partial t} + \frac{\partial(\rho_m u_m^2 + p)A}{\partial x} &= -p\frac{\partial A}{\partial x} \\
A\frac{\partial(\rho_m E_m)}{\partial t} + \frac{\partial(\rho_m u_m H_m A)}{\partial x} &= 0
\end{aligned}
\tag{1}
$$

Liquid phase

A liquid phase model, together with the appropriate thermodynamic relations (see equation (15)), is required to close the equation system (1). In this study, the choice has been made to use two different models. The first one is a simple and widely used two-equation model, assuming a mono-dispersion of the droplet sizes. The second one, namely the Quadrature Method of Moments, is mainly used for aerosol modelling, and only few authors used it for non-equilibrium condensation in wet steam (to the authors knowledge, the use of QMOM for wet steam flow has been presented only by Gerber and Mousavi (2007)). This model has the advantage of assuming several radii, so that a coarse spectrum can be computed.

Two-equation model

The mono-dispersed two-equation model has the advantages of simplicity, robustness and low computational cost.

$$\begin{aligned} \frac{\partial(\rho_m y)}{\partial t} + \frac{\partial(\rho_m u_m y)}{\partial x} &= \rho_m \left(N\dot{m}_l + m_{l,c}J\right) \\ \frac{\partial(\rho_m N)}{\partial t} + \frac{\partial(\rho_m u_m N)}{\partial x} &= \rho_m J \end{aligned} \tag{2}$$

The model is composed of two transport equations: the first one represents droplets mass conservation (the liquid mass fraction is transported) and the second stands for the conservation of the droplet number. The source term in the right hand side of the first equation represents the creation of mass due to the growth of the liquid phase (condensation around existing droplets) and the mass created by the appearance of new droplets in the flow. The source term in the right hand side of the second equation represents the creation of new droplets, J being the nucleation rate per unit mass of mixture. Finally, r_{2eq} is the mean radius, defined as:

$$r_{2eq} = \left(\frac{3}{4\pi\rho_l}\frac{y}{N}\right)^{1/3} \tag{3}$$

Quadrature Method of Moments

The Quadrature Method of Moments is a more advanced method. Here, the moments of the Particle Size Distribution (PSD) are tracked. The transport equation for the PSD incuding nucleation and growth can be written:

$$\frac{\partial(\rho_m f(r))}{\partial t} + \frac{\partial(\rho_m u_m f(r))}{\partial x} + \frac{\partial(\rho_m f(r) g(r))}{\partial r} = \rho_m J \delta_{r-r_c}, \tag{4}$$

$g(r)$ being the droplets growth law and $f(r)$ the distribution function. The full resolution of the PSD being complex and highly time consuming, only its first moments are transported. The moments can be written in integral form:

$$\mu_k = \int_0^\infty r^k f(r) dr \tag{5}$$

Combining equations (4) and (5), one can easily deduce an equation set based on the moments of the PSD, with $r^k f(r)$ vanishing for $r \to 0$ and $r \to \infty$ (White, 2003):

$$\frac{\partial(\rho_m \mu_k)}{\partial t} + \frac{\partial(\rho_m u_m \mu_k)}{\partial x} = k\rho_m \int_0^\infty r^{k-1} g(r) f(r) dr + \rho_m J r_c^k, \tag{6}$$

In the framework of the Standard Method of Moments (SMOM), the integrand on the right hand side of (6) is evaluated directly by assuming a constant, linear, or power-series growth law (White,

2003). Here, in the QMOM framework (McGraw, 1997), one can avoid those approximations on the growth law. The integrals is approximated by means of an n-point quadrature rule:

$$k\int_0^\infty r^{k-1}g(r)f(r)dr \cong k\sum_{i=1}^{n} r_i^{k-1}g(r_i)w_i \tag{7}$$

Using this quadrature rule, the growth law does not need to be integrated and any form can be used. The transport equations for the moments are written, using (4) and (7):

$$\frac{\partial(\rho_m\mu_k)}{\partial t}+\frac{\partial(\rho_m u_m\mu_k)}{\partial x}=\rho_m k\sum_{i=1}^{n} r_i^{k-1}g(r_i)w_i+\rho_m J r_c^k \tag{8}$$

The last issue with the QMOM method is the computation of the abscissas (i.e. radii) and weights (i.e. droplet number). Wheeler's algorithm (see orthog and gaucof subroutine from Press et al. (1992)), which has been succesfully compared with other methods such as the Product-Difference or the Golub-Welsch algorithms (John and Thein, 2012) is used in this paper. Using quadrature algorithms, $n/2$ abscissas and weights are computed using n moments. Due to the complexity of the algorithm (eigenvalues and eigenvectors of a tridiagonal $n*n$ matrix have to be found), this method is limited to reasonable numbers of weights and abscissas, otherwise precision and stability issues might occur. The liquid mass fraction and the average droplet radius are functions of the first moments:

$$r_{32}=\frac{\mu_3}{\mu_2} \qquad \text{and} \qquad y=\frac{4\pi\rho_l\mu_3}{3} \tag{9}$$

Condensation model and thermodynamic relations

Nucleation theory has been studied by many authors (see Bakhtar et al. (2005) for a review). In this study, classical, widely used, and up to date formulations have been used. The first parameter is the critical radius, which is the minimal radius to ensure the stability of the droplets in the flow:

$$r_c=\frac{2\sigma T_{sat}(p)}{\rho_l L_h(T_{sat}(p)-T_g)} \tag{10}$$

The number of droplets created during the nucleation process is defined by the nucleation rate, that is written per unit mass of mixture with ζ the Kantrowitz correction (Kantrowitz, 1951):

$$J=\frac{q_c}{1+\zeta}\left(\frac{2\sigma}{\pi m_*^3}\right)^{1/2}\frac{\rho_m}{\rho_l}exp\left(-\frac{4\pi r_c^2\sigma}{3k_BT_g}\right), \zeta=\frac{2(\gamma-1)}{\gamma+1}\frac{L_h}{R_{H_2O}T_g}\left(\frac{L_h}{R_{H_2O}T_g}-0.5\right) \tag{11}$$

Once the droplets are nucleated, they grow quickly. The growth law used for the two-equation and the QMOM methods is written (Young, 1982):

$$g(r)=\frac{dr}{dt}=\frac{\Lambda_g(1-r_c/r)(T_{sat}(p)-T_g)}{\rho_l r L_h\left(\frac{1}{1+2\beta K_n}+3.78(1-\nu)\frac{K_n}{P_r}\right)}, \tag{12}$$

with the correction factor ν given by:

$$\nu=\frac{R_{H_2O}T_{sat}(p)}{L_h}\left(\alpha-0.5-\frac{2-q_c}{q_c}\frac{\gamma+1}{2\gamma}\frac{c_pT_{sat}(p)}{L_h}\right) \tag{13}$$

Finally, the closure of the system is ensured by the thermodynamics of the gaseous phase, of the liquid phase, and the condensation model. The choice has been made to use the IAPWS-IF97 formulation

(IAPWS, 2007), with its extension to the metastable (or subcooled) region. Properties such as specific volume, entropy, enthalpy, etc. are given as functions of pressure and temperature. The temperature of the gaseous phase is given as a function of pressure and entropy (or enthalpy). For the liquid droplets, the evaluation of the temperature is given by:

$$T_l = T_{sat}(p) - (T_g - T_{sat}(p))\frac{r_c}{r} \tag{14}$$

Then, mixture properties are computed using the following relations, taking the liquid phase properties at the saturation temperature:

$$v_m = (1-y)v_g + yv_l, \quad e_m = (1-y)e_g + ye_l, \tag{15}$$

with

$$v_g(p, T_g), \quad v_l(p, T_{sat}(p)), \quad e_g(p, T_g), \quad e_l(p, T_{sat}(p)). \tag{16}$$

The relations (15) and (16) are also valid for enthalpy, entropy, and sound speed.

NUMERICAL TREATMENT

The first order finite volume discretization of equation systems (1) and (2) (or (1) and (8)) is performed using the $VFRoe_{ncv}$ scheme (Volumes-Finis-Roe with non-conservative variables) in a (s, u, p) formulation. This scheme solves a linearized Riemann problem, and is well suited for real gas Equation of State (Buffard et al., 2002). Furthermore, its implementation is relatively easy. Using a first order explicit Backward Euler temporal scheme, the evolution of the solution is written:

$$(W_i^{n+1} - W_i^n) + \frac{\Delta t}{\Delta x}\left(F_{i+1/2}^{num}(W_i^n, W_{i+1}^n) - F_{i-1/2}^{num}(W_{i-1}^n, W_i^n)\right) = 0; \tag{17}$$

The numerical fluxes are estimated using the exact fluxes at the intermediate states computed by the linearized Riemann problem. The properties transported within the condensation models (moments or liquid mass fraction and numbre of droplets) are treated as passive scalars, so that, taking only one passive scalar for notation simplicity (ψ), the eigenvalues for the Riemann problem are written: $\lambda_i = u_m + c, u_m, u_m - c, u_m$. Then, the intermediate states (Y_{int}) are computed following the rules:

$$Y_{int} = \begin{pmatrix} Y_l = Y_i, & \text{if } \lambda_1 > 0 & \Leftrightarrow & \bar{u} > \tilde{c} \\ Y_1, & \text{if } \lambda_1 \leq 0 \text{ and } \lambda_2 > 0 & \Leftrightarrow & 0 < \bar{u} \leq \tilde{c} \\ Y_2, & \text{if } \lambda_2 \leq 0 \text{ and } \lambda_3 > 0 & \Leftrightarrow & -\tilde{c} < \bar{u} \leq 0 \\ Y_r = Y_j, & \text{if } \lambda_3 \leq 0 & \Leftrightarrow & \bar{u} \leq -\tilde{c} \end{pmatrix} \tag{18}$$

Y_1 and Y_2 are written:

$$Y_1 = \begin{pmatrix} s_L \\ (u_n)_L \\ p_L \\ \psi_L \end{pmatrix} + \left(\frac{1}{2\bar{\nu}}[u_m]_L^R - \frac{1}{2\tilde{c}}[p]_L^R\right)\begin{pmatrix} 0 \\ \bar{\nu} \\ -\tilde{c} \\ 0 \end{pmatrix}, Y_2 = \begin{pmatrix} s_r \\ (u_n)_r \\ p_r \\ \psi_r \end{pmatrix} - \left(\frac{1}{2\bar{\nu}}[u_m]_L^R + \frac{1}{2\tilde{c}}[p]_L^R\right)\begin{pmatrix} 0 \\ \bar{\nu} \\ \tilde{c} \\ 0 \end{pmatrix} \tag{19}$$

In order to handle expansions across sonic points, linearized Riemann solvers need an entropy correction, otherwise non-physical shock waves might appear. When a sonic point is detected, the $VFRoe_{ncv}$ fluxes are replaced by (Helluy et al., 2010):

$$F^{num}(W_L, W_R) = F^{MVFRoe}(W_L, W_R) - \frac{min\left(|\lambda_k(W_L)|, |\lambda_k(W_R)|\right)}{2}(W_L, W_R) \tag{20}$$

The accuracy of the scheme, using the tabulated IAPWS-IF97 formulation for the thermodynamic, has been assessed with shock tube test cases, and compared with an exact solution (Blondel et al., 2013). The left and right states initial conditions for this test case are (1.0 bars, 1.66 m^3/kg, 0.0 m/s), respectively (1.5 bars, 3.33 m^3/kg, 0.0 m/s).

This test case is performed using a 12000 points mesh, which gives a good approximation of the solution. A detailed mesh study for shock tube tests, including first order convergence rates analysis, as well as a short description of the exact Riemann solver for real gases can be found in (Blondel et al., 2013). The results show that the expansion wave, the contact discontinuity and the shock wave are well caught, showing the validity of the $VFRoe_{ncv}$ scheme (figures (1) and (2)).

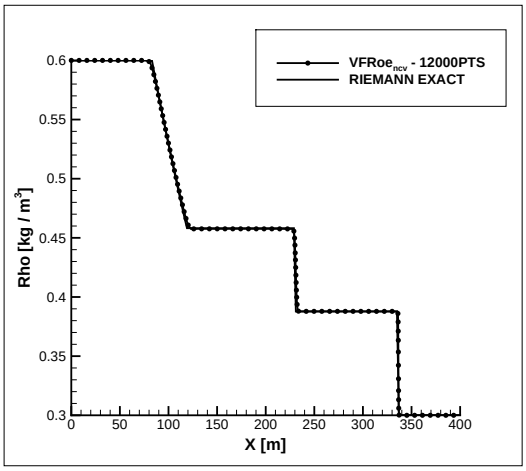

Figure 1: $VFRoe_{ncv}$ **and exact solution in a shock tube (density)**

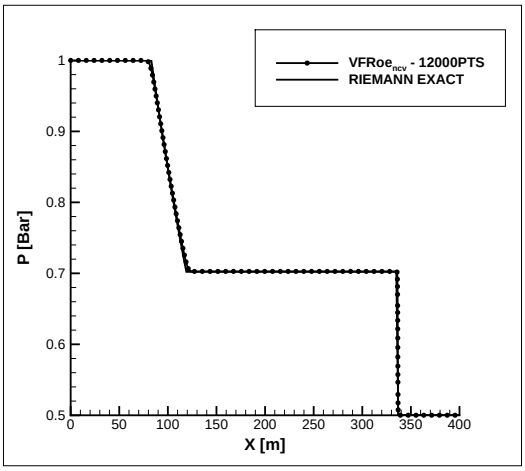

Figure 2: $VFRoe_{ncv}$ **and exact solution in a shock tube (pressure)**

RESULTS

During the validation process, the QMOM method has been used with a set of 12 moments, leading to 6 computed radii. Higher number of moments can be transported, but it often leads to abscissas of zero-weights that are useless. Another issue is that the flow is dry at the inlet of the nozzle, and quadrature algorithm can not succeed if the moments are zero (Machisio and Fox, 2005). To overcome this issue, two main techniques can be used: particles can be injected at the inlet, so that moments are non-zero in the all domain, or, if no particles are injected at the inlet, the flow can be initialized with a guess distribution, so that when nucleation appear, moments are non-zeroes. For all calculations introduced below, the second technique has been used. A mesh study has been done in order to minimize the error on the prediction of the droplet sizes, that can be huge for coarse meshes (Blondel et al., 2013). Uniform 4000 cells meshes have been used for all steady and unsteady calculations below, which is a good compromise between results accuracy and computational time for the first order numerical integration used here.

Steady nozzle flow

The first validation case is the well-known Moore's nozzle (Moore et al., 1973). Nozzle B is used, with 0.25 bar and 358.15 K for the stagnation pressure and temperature conditions at the inlet.

The expansion is well caught by the two methods (figure 3). The Wilson point (the point where nucleation occurs) is exactly at the same position, but droplets grow faster with the QMOM compared with the two-equation model, involving a stronger pressure drop. This difference is not surprising, as

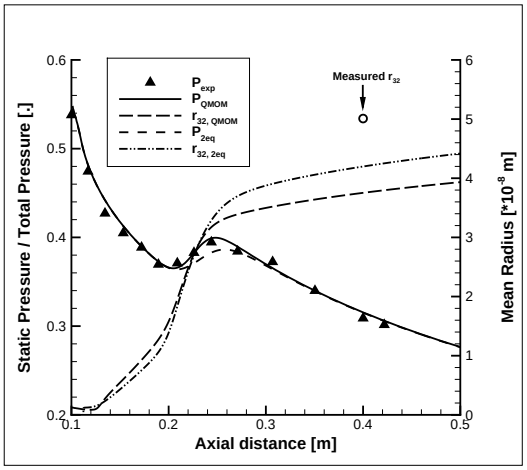

Figure 3: **Pressure expansion and mean droplet sizes in the Moore's nozzle - Comparison with experimental data**

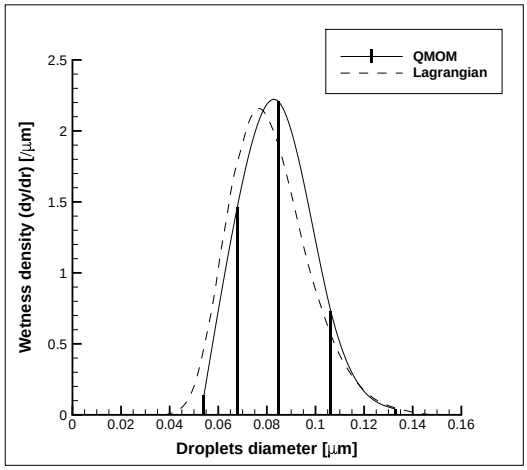

Figure 4: **Radius distribution at the outlet of the Moore's nozzle - Comparison with a Lagrangian calculation (White, 2003)**

the growth is estimated at the mean radius (r_{2eq}) in the two-equation model, whereas it is estimated with the computed abscissas (r_i) with the QMOM method. Thus, the predicted average radii are slightly different (figure 3). The results are still good with both methods, predicting an average radius of 0.0385 μm for the QMOM and 0.0475 μm for the two-equation model, which is close to the experimental radius (0.05 μm). Moreover, the comparison between the distribution computed with the QMOM method and a reference distribution computed with a Lagrangian model (White, 2003) is very good. The distributions have the same shape (using a spline interpolation between the six weights for the QMOM method) and the contribution to wetness fraction are very close. The numerical treatment adopted in (White, 2003) is different than the one adopted here (centered, second order scheme and 4-stage Runge-Kutta time integration) and might also be a source of differences in the numerical results.

Steady and shocked nozzle flow

The second validation case is a steady state flow, with a shock wave induced by a critical heat release in the diverging part of the nozzle (Barschdorff, 1970). There are no droplet size measurements available, so that only the static pressure can be compared with the experiment. The stagnation pressure and temperature are respectively 0.784 bar and 373.15 K at the inlet.

With the two-equation model, the pressure expansion has a small error with respect to experimental data, nucleation appearing upstream the measurements. The QMOM method fits much better the experimental data. The value of the mean radius at the nozzle outlet is very different between the two methods. This had already been highlighted for the same test case between the two-equation model and a bi-fluid model (Dykas and Wroblewski, 2011). There are two main reasons for those differences: first, using the QMOM, the growth of the liquid phase is based on the six computed abscissas and not on the mean radius. Secondly, the definition of the average radius is not the same in the two models (see equations (3) and (9)). The differences observed in this computationnal case highlight an overprediction of the average droplet size using the two-equation model, leading to a condensation shock appearing very soon in the nozzle.

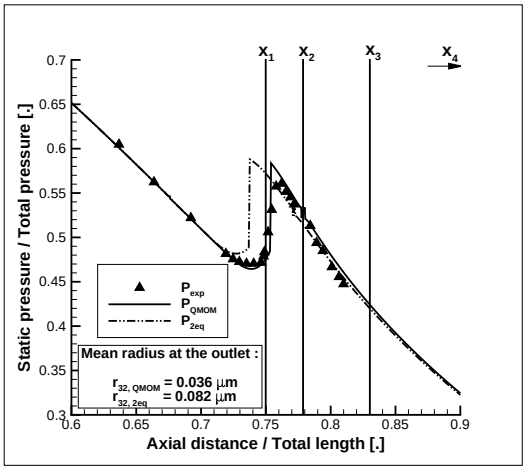

Figure 5: **Expansion in the Barschdorff's nozzle, comparison with experimental data**

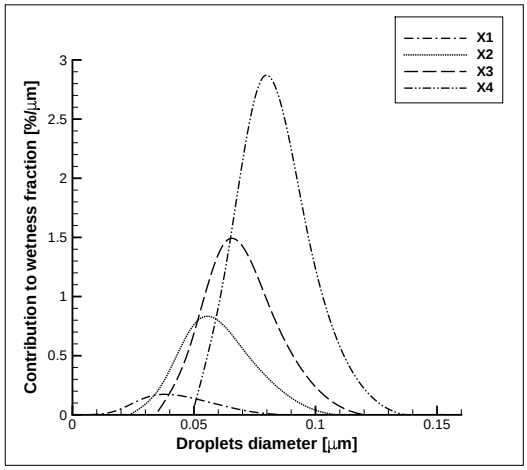

Figure 6: **Droplet spectrum at four axial positions in the Barschdorff's nozzle**

Unsteady and shocked nozzle flow

The last validation case deals with an unstable shock wave moving through the throat, due to super-critical heat addition (nozzle 1 from Dorey et al., (2010)). The stagnation pressure and temperature at the inlet are: 1.3 bar and 382.15 K. Only the frequency of the instability has been measured using a high speed camera. The agreement between the measured ($1170Hz$) and the computed frequencies is good for the two methods: 1% for the two-equation model ($1161Hz$) and 4% for the QMOM ($1220Hz$).

The evolution of the droplet spectrum taken at the outlet (figure 7) highlights the ability of QMOM to represent the polydispersion under critical flow conditions, such as quickly evolving spectrum and shock waves. Droplets are generated in a large interval of radii: 0.05 μm to 0.2 μm. When the shock wave is strong (instants T1 and T2, figure 7), small droplets are created: the nucleation rate is high, leading to a large number of nucleated droplets of small sizes. When the shock is disappearing in the converging part of the nozzle, nucleation being less intense (the shock wave travelling through the throat induces a temperature jump, and thus a smaller subcooling downstream), less droplets, but of bigger sizes, are created (instant T3). Then, the heat release being sup-critical, a new cycle begins, with a shock-wave moving toward less subcooled regions of the flow. The evolution of the

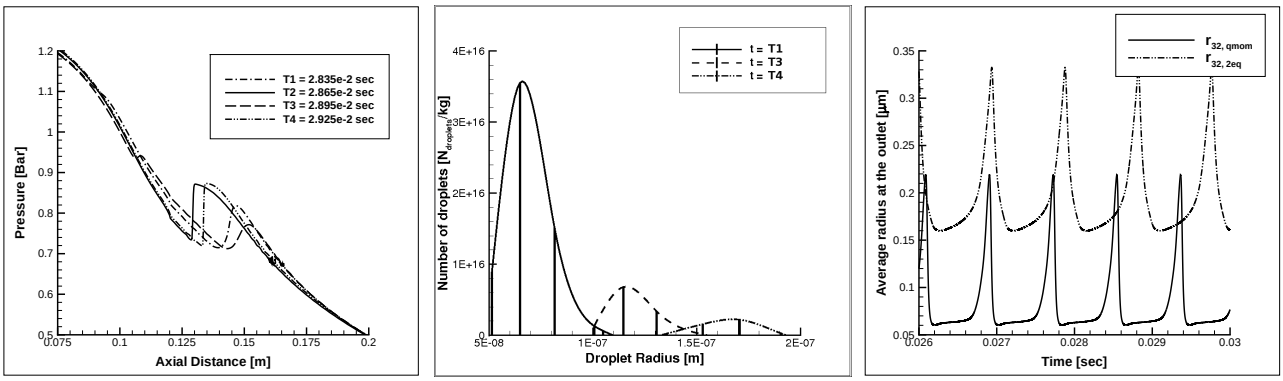

Figure 7: **Pressure expansion and droplet spectra (QMOM), outlet radii (2eq, QMOM)**

average droplet radii, r_{2eq} and r_{32}, shows that once again, both methods give different results (figure

7). However, the predicted evolution is very similar in both methods, with a peak of large droplets and a plateau of small droplets during each instability cycles.

Application to a 3D/1D chained calculations

The final calculation run to test the ability of the QMOM to deal with realistic phenomena occuring in turbines is a chained calculation between a 3D, perfect gas Navier-Stokes solver and the 1D real gas code. The flow in a nuclear power plant low-pressure steam turbine stage where the nucleation is supposed to appear has been computed using an unsteady chorochronical method (see Stanciu et al., 2010). The flow in the 3D calculation is subsonic and highly unsteady due to the blade passage effects. The involved frequencies are high (around 5700 Hz). Then, pressure and temperature signals have been extracted and imposed at the inlet of an EDF's nozzle (nozzle 3 from Dorey et al., 2010), in order to predict the nucleation under such unsteady flow conditions and assess the capability of the QMOM method to robustly deal with.

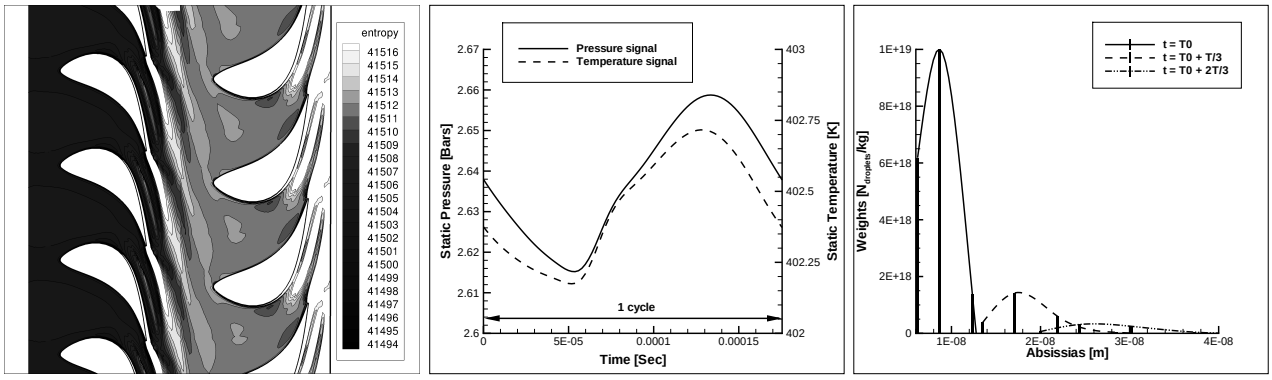

Figure 8: **3D unsteady entropy field in a turbine stage, nozzle unsteady inlet signals and droplet spectrum evolution during one period**

The evolution of the droplet spectrum is caught by the QMOM method (figure 8), even with a highly unsteady inlet signal, with strong pressure variations: the spectra computed here are broad, ranking from 0.005 μm to 0.05 μm. The QMOM method clearly add new information in the computations, that are very useful to understand the nucleation occuring in steam turbines. Also, using this method can improve significantly the prediction of other phenomena, such as deposition and liquid film behaviour on blades, which are sensitive to droplet sizes and spectra (Fendler et al., (2012)).

CONCLUSIONS

The Quadrature Method of Moments has been tested through academic supersonic nozzle cases in order to assess its ability to handle unsteady flows with strong variations and discontinuities, such as trailing edge wakes and shock waves. A first chained 3D / 1D calculation has been run, showing the ability of the method to handle complex physics. The robustness of the method is as good as of the classical two-equation model. Even if only 6 abscissas and weights are computed, the comparison with Lagrangian style calculations has proven the interest and the validity of the method. For a low additional computational cost, the QMOM gives richer information on droplet spectra.

The lack of experimental data on specta in nozzles is a hindrance to the complete validation of the method. Experiments will be carried out in collaboration with the ITSM (Institute of Thermal Turbomachinery and Machinery, Stuttgart University) to propose complete and up to date validation cases, with droplet spectra measurements.

The QMOM methodology is currently being improved with second order schemes and implemented in the 3D CFD code *elsA* in order to treat larger and 3D configurations.

REFERENCES

Anderson J.D., (1995), Computational Fluid Dynamics : The basics with applications, McGraw-Hill.

Bakhtar F., Young J.B., White A.J., Simpson D.A., (2005), Classical nucleation theory and its application to condensing steam flow calculations, Proc. of the IMechE., Vol. 219 pp. 1315-1333.

Barschdorff D., (1970), Droplet formation, influence of shock waves and instationary flow patterns by condensation phenomena at supersonic speeds, 3^{rd} Conf. On Rain Erosion, 691-705.

Blondel F., Audebert B., Pasutto T., Stanciu M., (2013), Condensation models and boundary conditions for non-equilibrium wet steam flows, Int. J. of Finite Volumes, In Press.

Buffard T., Gallouët T., Hérard J. M., (2000), A sequel to a rough Godunov scheme: Application to real gases. Comp. and Fluids, Vol. 29 pp. 813-847.

Dorey J.M., Stanciu M., Ren K., (2010), Experiments on steam condensation in a 3-scale nozzle vein using light extinction and a high speed camera. 7th Int. Conf. on Multiphase Flows.

Dykas S., Wróblewski W., (2011), Single- and two-fluid models for steam condensing flow modeling. Int. J. of Multiphase Flow, Vol. 37 pp. 1245-1253.

Fendler Y., Dorey J.M., Stanciu M., Lance M., Leonard O., (2012), Developments for modeling of droplets deposition and liquid film flow in a throughflow code for steam turbines, ASME 2012.

Gerber A. G., Mousavi A., (2007), Application of the Quadrature-Method-of-Moments to the polydispersed droplet spectrum in transonic steam flows with primary and secondary nucleation. J. Appl. Math. Modelling, Vol. 31 pp. 1518-1533.

Helluy P., Hérard J.M., Mathis H., Müuller S. , (2010), A simple parameter-free entropy correction for approximate Riemann solvers. C.R. Mecanique, Vol. 338 pp. 493-498.

IAPWS 97, (2007), Revised release on the IAPWS industrial formulation 1997 for the thermodynamic properties of water and steam.

John V., Thein F., (2012), On the efficiency and robustness of the core routine of the quadrature method of moments (QMOM), Chemical Eng. Science, Vol. 75 pp. 327-333.

Kantrowitz A., (1951), Nucleation in very rapid vapor expansions. J. of Chem. Physics, Vol. 19.

McGraw R., (1997), Description of aerosol dynamics by the quadrature method of moments. Aerosol Sci. and Tech., Vol. 27 pp. 255-265.

Marchisio D.L., Fox .R.O., (2005), Solution of population balance equations using the direct quadrature method of moments, Aerosol Science, Vol. 36, pp. 43-73.

Moore M., Walters P., Crane R., Davidson B., (1973), Predicting the fog-drop size in wet steam turbines, Instn. Mesh. Eng. Conf. pub. Heat and Fluid Flow in Steam and Gas Turbine Plant., 101-109

Press W.H., Teukolsky S.A., Vetterling W.T., Flannery B.P., (1992), Numerical Recipes in Fortran, Second Edition, Cambridge University Press

Stanciu M., Fendler Y., Dorey J.M., (2011), Unsteady stator-rotor interaction coupled with exhaust hood effect for last stage steam turbines, European Turb. Conf.

White A. J., (2003), A comparison of modelling methods for polydispersed wet steam flow. Int. J. Numer. Meth. Engng, Vol. 57 pp. 819-834.

Young J.B., (1982), The spontaneous condensation of steam in supersonic nozzles. PhysicoChemical Hydrodynamics, Vol. 3, pp 57-82.